

Galaxy Formation in Preheated Intergalactic Media

H.J. Mo¹, Shude Mao² ^{*}

¹*Max-Planck-Institut für Astrophysik Karl-Schwarzschild-Strasse 1, 85748 Garching, Germany*

²*Jodrell Bank Observatory, Macclesfield, Cheshire SK11 9DL, UK*

Accepted Received; in original form

ABSTRACT

We outline a scenario of galaxy formation in which the gas in galaxy-forming regions was preheated to high entropy by vigorous energy feedback associated with the formation of stars in old ellipticals and bulges and with AGN activity. Such preheating likely occurred at redshifts $z \sim 2 - 3$, and can produce the entropy excess observed today in low-mass clusters of galaxies without destroying the bulk of the Ly α forest. Subsequent galaxy formation is affected by the preheating, because the gas no longer follows the dark matter on galaxy scales. The hot gas around galaxy haloes has very shallow profiles and emits only weakly in the X-ray. Cooling in a preheated halo is not inside-out, because the cooling efficiency does not change significantly with radius. Only part of the gas in a protogalaxy region can cool and be accreted into the final galaxy halo by the present time. The accreted gas is likely in diffuse clouds and so does not lose angular momentum to the dark matter. Cluster ellipticals are produced by mergers of stellar systems formed prior to the preheating, while large galaxy disks form in low-density environments where gas accretion can continue to the present time.

Key words: galaxies: formation - galaxies: structure - galaxies: spiral - galaxies: elliptical - galaxies: clusters

1 INTRODUCTION

In the past 20 years, the Cold Dark Matter (CDM) cosmogony (Peebles 1982; Blumenthal et al. 1984) has become the most appealing scenario for the formation of structure in the universe. In the CDM cosmogony, the universe is assumed to be dominated by CDM, and the structure in the universe forms in a hierarchical fashion, with dark matter particles aggregating into larger and larger clumps (dark haloes) in the passage of time. In this scenario, galaxies are assumed to form as gas cools and condenses in dark haloes (White & Rees 1978), and the properties of galaxies are determined by the properties of their host haloes, such as mass, density profile, angular momentum, and merging history. This standard scenario of galaxy formation has been quite successful in predicting many of the observed properties of the galaxy population, such as disk sizes and kinematics (e.g. Fall & Efstathiou 1980; Dalcanton, Spergel & Summers 1997; Mo, Mao & White 1998, hereafter MMW; Avila-Reese, Firmani & Hernandez 1998; Heavens & Jimenez 1999; Mo & Mao 2000; Navarro & Steinmetz 2000; van den Bosch 2000), and the distributions of luminosity, colour and morphology

(e.g. White & Frenk 1991; Kauffmann, White & Guiderdoni 1993; Cole et al. 1994; Somerville & Primack 1999).

One key ingredient in the standard scenario is a mechanism which can prevent gas from cooling too fast in dark matter haloes, because without such a mechanism, we may run into the following set of problems.

- The overcooling problem: In a hierarchical model, all dark matter was in small haloes at high redshifts. Since radiative cooling of gas in these haloes is effective, all the gas would have cooled and formed stars, leaving no gas for producing quasar absorption line systems and for the formation of galaxy disks at low redshifts. This is the ‘overcooling problem’ first pointed out by White & Rees (1978).
- The baryon-fraction problem: Based on cosmic nucleosynthesis (e.g. O’Meara et al. 2001) and Cosmic Microwave Background Radiation (e.g. de Bernardis et al. 2002), the baryon density in the universe is $\Omega_{B,0} \approx 0.02h^{-2}$. For a universe with $\Omega_0 \approx 0.3$ and $h \approx 0.7$, the implied overall baryon fraction is about $f_B \equiv \Omega_{B,0}/\Omega_0 \approx 0.13$, consistent with the baryon fraction in rich clusters (e.g. White et al. 1993; Ettori & Fabian 1999). On the other hand, modelling of galaxy disk formation in CDM haloes showed that the gas mass which settles into the disk is only $\sim 5\%$ of the total halo mass and a much higher fraction would produce disks which might be unstable and have too peaked rotation curves (e.g. MMW).

^{*} E-mail: hom@mpa-garching.mpg.de, smao@jb.man.ac.uk

Since the total amount of hot gas in a galaxy halo is small, a consistent model of disk formation requires that only part of the gas in a protogalaxy region ends up in the final halo. The question is then what regulates the baryon fraction in galaxy haloes.

- Angular-momentum problem: Since gas can cool rapidly in small progenitor haloes to form condensed central objects, it can lose most of its angular momentum to the dark matter during galaxy assembly (e.g. Navarro & White 1994). This leads to serious problems when comparing with real galaxies: the disks formed in this way are too small.

- X-ray halo problem: In the standard scenario, gas in a galactic halo is assumed to be shock-heated to the virial temperature (which is about 10^6 K) by gravitational collapse, and (massive) galactic haloes are predicted to emit in X-ray, with a bolometric luminosity of the order 10^{42} erg s $^{-1}$. The predicted luminosity is about one order of magnitude higher than what is observed in the haloes of spiral galaxies (e.g. Benson et al. 2000). This is a well-known problem (e.g. White & Frenk 1991) but has been largely ignored in theoretical studies of galaxy formation so far.

Two mechanisms have been proposed to solve these problems. The first is photoionization heating of the intergalactic medium (IGM) by the UV background. Detailed analyses showed that photoionization heating is effective in prohibiting gas cooling only in small haloes, with circular velocity $V_c \lesssim 50$ km s $^{-1}$ (e.g. Efstathiou 1992; Gnedin 2000). Thus, while photoionization heating may be able to keep some of the IGM in a diffuse form (and so alleviating the overcooling problem), its effect on gas assembling and cooling in galactic haloes may not be sufficient to solve the other problems mentioned. The second possibility is heating by the energy feedback from star formation (Larson 1974; White & Rees 1978; Dekel & Silk 1986). In many semi-analytic models of galaxy formation (e.g. White & Frenk 1991; Kauffmann et al. 1993; Cole et al. 1994; Somerville & Primack 1999; Kauffmann et al. 1999), this feedback is implemented in such a way that the gas in galactic haloes is assumed to be effectively heated by supernova explosions associated with the star formation in the galaxy, and the heated gas is assumed either to be retained within the halo or ejected from the halo to some larger scale. Detailed modelling showed that the total energy feedback from supernova explosions in a galaxy is sufficient to keep a large amount of gas at a high temperature, and the feedback efficiency can be tuned to reproduce many of the observed properties of the galaxy population. Unfortunately, our understanding of such feedback is still very limited, and it is unclear how it operates in detail.

In this paper, we consider another possible implementation of the feedback process. We assume that the IGM in galaxy-forming regions was heated to some high entropy at some high redshift during an early period of vigorous star formation and associated AGN activity. We examine the effect of such preheating on subsequent galaxy formation. This implementation is motivated by three lines of observational evidence. (i) Observations show that many stars in the universe may have formed at $z \gtrsim 2$ in systems reminiscent of local starburst galaxies (see Heckman 2001 and references therein). Such galaxies can produce supernova-driven outflows which may be able to heat the IGM in the surrounding

regions. (ii) The comoving number density of AGNs is highest around redshifts $z = 2 - 3$ (Shaver et al. 1996). Since a lot of kinetic energy can be released from AGNs, the surrounding IGM can be heated to a high temperature, if some of this kinetic energy is thermalized (e.g. Inoue & Sasaki 2001). (iii) Observations of X-ray clusters and groups suggest that there is an entropy excess in these systems relative to that expected from gravitational collapse alone (e.g. Ponman, Cannon & Navarro 1999; Lloyd-Davies et al. 2000). This can be explained if the IGM in protocluster (protogroup) regions was preheated to a high temperature (e.g. Ponman et al. 1999; Tozzi & Norman 2001). The implementation considered here is related to some of the early implementations (e.g. Nulsen & Fabian 1995, 1997; Sommer-Larsen, Gelato & Vedel 1999), but has some distinct properties. We emphasize the importance of early starbursts and associated AGN activity, and we consider heating of the gas while it was still in diffuse form outside galactic haloes. Furthermore, our model presents more detailed discussions about the properties of the preheated gas in connection to the puzzling features of observed galaxies mentioned above.

Preheating affects subsequent galaxy formation because the heated gas cannot collapse into small dark haloes and so no longer follows the bottom-up clustering hierarchy of the dark-matter component. We show that the introduction of preheating can help to solve some of the problems mentioned above. The paper is structured as follows. In Section 2, we describe our assumptions on the properties of the preheated IGM and analyze gas cooling and accretion onto dark haloes in such a medium. The formation of galaxies in the present scenario is described in Section 3. In Section 4, we discuss briefly how the IGM may have been preheated. Further discussion of the present model and a summary of our main conclusions are given in Section 5. Throughout this paper, when necessary, we adopt the standard Λ CDM cosmogony, with matter density $\Omega_0 = 0.3$, a cosmological constant corresponding to $\Omega_\Lambda = 0.7$, and a normalization $\sigma_8 = 0.9$ for the power spectrum. We write the Hubble constant as $H_0 = 100h$ km s $^{-1}$ Mpc $^{-1}$ and take $h = 0.7$.

2 GAS ACCRETION BY DARK HALOES IN A PREHEATED INTERGALACTIC MEDIUM

2.1 The preheated IGM

For a (completely ionized) cosmic gas, the mean number density of electrons at redshift z is

$$\bar{n}_e \approx 2.0 \times 10^{-7} \left(\frac{\Omega_{B,0} h^2}{0.02} \right) (1+z)^3 \text{ cm}^{-3}, \quad (1)$$

where $\Omega_{B,0}$ is the cosmic density parameter of baryons, and $\Omega_{B,0} h^2 \sim 0.02$ as given by cosmic nucleosynthesis (e.g. O’Meara et al. 2001). Now consider a volume in which the electron density is $n_e = \bar{n}_e(1+\delta)$ and the temperature is T . We define an entropy parameter as

$$\mathcal{S} \equiv \frac{T}{n_e^{2/3}}, \quad (2)$$

where it is conventional to express the temperature in units of keV (1 keV corresponds to $T \approx 1.2 \times 10^7$ K). If the gas is adiabatic, then \mathcal{S} is conserved and the temperature of the gas can be written in terms of \mathcal{S} as

$$T = 4.4 \times 10^4 S_{100} (1 + \delta)^{2/3} (1 + z)^2 \text{ K}, \quad (3)$$

where

$$S_{100} \equiv \left(\frac{\mathcal{S}}{100 h^{-1/3} \text{ keV cm}^2} \right) \left(\frac{\Omega_{B,0} h^2}{0.02} \right)^{2/3} h_{0.7}^{-1/3}, \quad (4)$$

$h_{0.7} \equiv h/0.7$. Note that the h dependence at the end of the equation appears because the observed value of \mathcal{S} has such a dependence. For a given \mathcal{S} the required temperature is lower if the gas density is lower. For example, if $S_{100} = 1$ and if preheating was at $z = 3$ in the mean medium ($\delta = 0$), the required temperature would be $T \sim 7.5 \times 10^5 \text{ K}$. If, on the other hand, heating is in the central region of a present-day cluster, where $\delta \sim 10^4$, the required temperature would be $T \sim 2 \times 10^7 \text{ K}$.

The time-scale of radiative cooling, defined as $t_{\text{cool}} \equiv T/\dot{T}$, can be written as

$$\begin{aligned} t_{\text{cool}} &\approx \frac{3kT\mu_i}{2\mu_e\Lambda(T)} \\ &\sim 1.0 \times 10^{11} \Lambda_{-23}^{-1} T_6 \left(\frac{\Omega_{B,0} h^2}{0.02} \right)^{-1} \\ &\quad \times (1 + \delta)^{-1} \left(\frac{1 + z}{4} \right)^{-3} \text{ yr}, \end{aligned} \quad (5)$$

where $T_6 \equiv T/10^6 \text{ K}$, $\mu \approx 0.6$ and $\mu_i \approx 1.2$ are the mean molecular weights per particle and per ion, respectively, and Λ_{-23} is the cooling function $\Lambda(T)$ in units of $10^{-23} \text{ cm}^3 \text{ erg s}^{-1}$ as defined in Sutherland & Dopita (1993). Notice that μ_i enters because Sutherland & Dopita (1993) defines the cooling rate per unit volume as $n_e n_i \Lambda(T)$, where n_i is the total ion density. If we approximate the cooling function as a power law of gas temperature, $\Lambda(T) \propto T^{-\alpha}$, the cooling time in an approximately isentropic gas scales as

$$t_{\text{cool}} \propto \frac{T}{n_e \Lambda(T)} \propto T^{\alpha-1/2} \propto n_e^{2(\alpha-1/2)/3}. \quad (6)$$

Thus, depending on whether $\alpha > 1/2$ or $\alpha < 1/2$, the cooling time is longer or shorter for a high-density (high-temperature) gas. This is different from an isothermal gas, where t_{cool} is always shorter for higher n_e .

The cooling time given above should be compared to the Hubble time

$$t_H = 3.2 \times 10^9 h_{0.7}^{-1} \left(\frac{\Omega_0}{0.3} \right)^{-1/2} \left(\frac{1 + z}{4} \right)^{-3/2} \mathcal{H}(z) \text{ yr}, \quad (7)$$

where $\mathcal{H}(z) \equiv \Omega_0^{1/2} (1 + z)^{3/2} H_0 / H(z)$. Note that $\mathcal{H}(z) \sim 1$ for $z \gtrsim 1$ in a flat universe with $\Omega_0 \sim 0.3$. As one can see, cooling is ineffective at low overdensities and at low preheating redshift ($z \lesssim 3$). In this case, the specific entropy \mathcal{S} is approximately conserved (except in shocks), and the evolution of the temperature is given by equation (3). The properties of the preheated gas are then specified by its density [which is proportional to $(1 + \delta)(1 + z)^3$] and the value of \mathcal{S} .

One way to specify the initial entropy is to use the observed entropy excess in clusters and groups (Ponman, Cannon & Navarro 1999; Lloyd-Davies et al. 2000), which gives $\mathcal{S} \sim 100 \text{ keV cm}^2$. We use this as the fiducial value for \mathcal{S} . It must be emphasized, however, that in reality the value of \mathcal{S} may change from place to place, but we ignore this complication here.

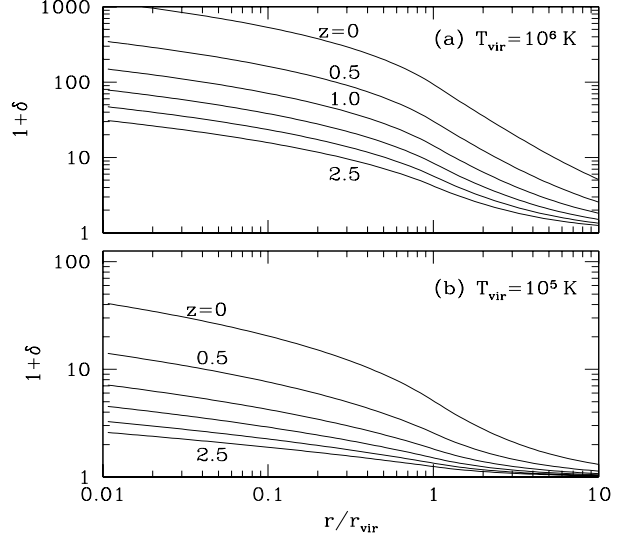


Figure 1. Density profiles of preheated gas (assumed to be adiabatic, with $S_{100} = 1$) as a function of radius around dark haloes. Six curves are shown for redshift from 0 to 2.5 with a step size of 0.5. Results are shown for (a) a normal galaxy halo with $T_{\text{vir}} = 10^6 \text{ K}$ and (b) a dwarf galaxy halo with $T_{\text{vir}} = 10^5 \text{ K}$.

In Section 4, we will discuss in some detail how the IGM may have been preheated. Based on the discussion there, we advocate a preheating process which can be summarized as follows:

- The preheating was due to the starbursts (and associated AGN activity) responsible for the formation of old stars in ellipticals and bulges.
- The preheating was likely to be confined to protocluster and protogroup regions where starbursts were common.
- Although preheating must be a continuous process and different regions may have been preheated at different times, the bulk of preheating was likely to be around a redshift $z \sim 2 - 3$, where the star-formation rate and AGN number peak.

The details of the preheating process are still poorly understood, but much of the following discussion is independent of these details.

2.2 Accretion of the hot IGM

Consider a dark halo with mass M_{vir} , circular velocity V_c , virial temperature T_{vir} , and virial radius r_{vir} . According to the spherical collapse model, these quantities are related as follows:

$$M_{\text{vir}} = \frac{V_c^3}{10GH(z)}, \quad r_{\text{vir}} = \frac{V_c}{10H(z)}, \quad T_{\text{vir}} = \frac{\mu m_p V_c^2}{2k}. \quad (8)$$

The virial temperature is the same as the isothermal temperature for a singular isothermal sphere, but its meaning is less clear for more complex halo profiles. It should only be regarded as an approximate measure of the gas temperature in the halo. We model the dark matter halo as a singular isothermal sphere with density profile

$$\rho(r) = \frac{V_c^2}{4\pi G r^2}. \quad (9)$$

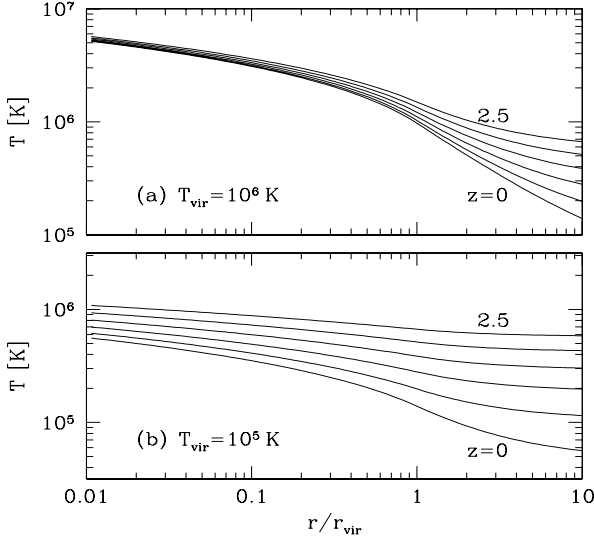


Figure 2. Temperature profiles of preheated gas (assumed to be adiabatic, with $S_{100} = 1$) as a function of radius around dark haloes. Results are shown for (a) a normal galaxy halo with $T_{\text{vir}} = 10^6$ K and (b) a dwarf galaxy halo with $T_{\text{vir}} = 10^5$ K.

In a preheated medium where gas cooling is unimportant, the halo can accrete the preheated gas through adiabatic compression. If the gas accretion is subsonic (Tozzi, Scharf & Norman 2000), then we may solve for the distribution of gas within the halo as follows. Assuming spherical symmetry and hydrostatic equilibrium (the latter assumption is valid in a region where the sound-crossing time is much shorter than the age of the universe), we have

$$\frac{1}{\rho} \frac{dP}{dr} = -\frac{GM}{r^2}, \quad (10)$$

where ρ and P are the density and pressure of the gas at radius r , M is the mass within radius r . For the gas outside the halo, we may take M to be the total mass of the halo. If the gas is not significantly shocked when establishing the hydrostatic equilibrium, as is the case if the temperature of the preheated gas is not much lower than the virial temperature of the halo, the specific entropy $T/n_e^{2/3}$ will remain at the preheated value \mathcal{S} . In this case, the hydrostatic equilibrium equation can be solved for the gas density:

$$n^{2/3} = \frac{2}{5} \frac{GM_{\text{vir}} \mu m_p}{k\mathcal{S}} \frac{1}{r} + \text{constant}. \quad (11)$$

Assuming that n is equal to the mean density at $r \rightarrow \infty$, and using the relation between halo mass and halo virial temperature, we have

$$n^{2/3}(r) = \bar{n}^{2/3} + \frac{4}{5} \frac{T_{\text{vir}}}{\mathcal{S}} \frac{r_{\text{vir}}}{r}, \quad (r \geq r_{\text{vir}}). \quad (12)$$

We caution that equation (12) is only approximate at large radii as the gas is likely not in hydrostatic equilibrium. Within the virial radius of an isothermal sphere, the hydrostatic equilibrium of adiabatic gas leads to the following profile:

$$n^{2/3}(r) = \bar{n}^{2/3} + \frac{4}{5} \frac{T_{\text{vir}}}{\mathcal{S}} \left(1 - \ln \frac{r}{r_{\text{vir}}}\right), \quad (r < r_{\text{vir}}). \quad (13)$$

The corresponding temperature profile is given by

$$T(r) = \mathcal{S} n^{2/3}(r). \quad (14)$$

Some examples of the density and temperature profiles are shown in Figures 1 and 2. As one can see, the density profile is very shallow. In fact this is the shallowest equilibrium profile one can get in a singular isothermal sphere, because any shallower profile is convectively unstable.

2.3 X-ray emission from galactic haloes

Given the density and temperature profiles, we can estimate the radiation luminosity of the hot gas in a dark halo. Since the temperature of the gas is about 0.1 keV for a galaxy halo, the radiation is in the soft X-ray band, and we can hope to detect such emission through X-ray observations. The bolometric X-ray surface brightness is given by

$$S_X(R) = \frac{1}{4\pi} \int \Lambda[T(r)] n_e n_i dy, \quad (15)$$

where $r = (R^2 + y^2)^{1/2}$, and R is the radius in projection. The luminosity within a radius, $L_X(< R)$, can then be obtained by integrating S_X over area and solid angle. Figure 3 shows $S_X(R)$ and $L_X(< R)$ for a present-day galactic halo with virial temperature $T_{\text{vir}} = 10^6$ K, corresponding to $V_c \approx 170 \text{ km s}^{-1}$. In the calculation, we have taken a metallicity $Z = 0.1 Z_\odot$ and neglected the contribution of the gas outside the virial radius of the halo as the gas temperature becomes too low to be in the X-ray band (see Fig. 2). For simplicity, we have also assumed that all the gas is in the hot phase. As one can see, the predicted X-ray emission depends significantly on the assumed specific entropy: a higher value of S_{100} leads to a less concentrated gas distribution and so to lower X-ray surface brightness and luminosity. For $S_{100} = 1$, the surface brightness at $R = 100$ and 20 kpc are $S_X \sim 2.5 \times 10^{-9}$ and $5 \times 10^{-9} \text{ erg s}^{-1} \text{ cm}^{-2} \text{ sr}^{-1}$, respectively. The total luminosity within the virial radius is $L_X \sim 3 \times 10^{40} \text{ erg s}^{-1}$. These predicted surface brightness and luminosity are about a factor of 10 smaller than what one obtains based on the assumption that gas in galactic haloes is shock-heated to the virial temperature and in hydrostatic equilibrium in the dark-halo potential (e.g. White & Frenk 1991; Benson et al. 2000), because of the shallower gas density profiles.

It should be pointed out that the results obtained here are valid only for isolated late-type galaxies. For galaxies in clusters and groups, the X-ray emission may be affected by the intracluster (intragroup) medium. For elliptical galaxies which contain many stars, the interaction between supernova-driven winds and gas accretion may also play an important role in the formation of X-ray haloes (e.g. Brighenti & Mathews 1999). Thus, the most relevant observational results to compare our model predictions with are those obtained by Benson et al. (2000) for the diffuse X-ray emission from 3 late-type galaxy haloes. The upper limits on the bolometric luminosities of these three haloes are of the order $10^{41} \text{ erg s}^{-1}$. These observational results are consistent with our model prediction, if the circular velocities of these haloes (at virial radius) are $V_c \sim 200 \text{ km s}^{-1}$. If the circular velocities of these galaxies were as high as the measured rotation velocities of the disks ($\sim 300 \text{ km s}^{-1}$, corresponding to a virial temperature of about 0.3 keV), shock heating of the gas by gravitational accretion becomes significant. Cal-

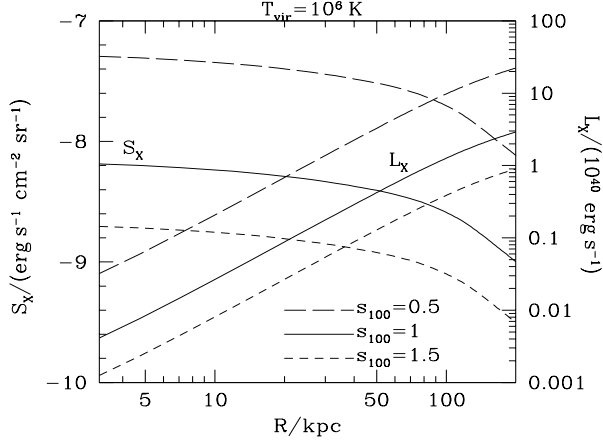


Figure 3. The X-ray surface brightness $S_X(R)$ and luminosity $L_X(<R)$ (within radius R) of the hot gas around a present-day galactic halo with virial temperature $T_{\text{vir}} = 10^6$ K. Results are shown for three different values of S_{100} .

culations by Tozzi & Norman (2001) including this effect give an X-ray luminosity of $\sim 10^{41} \text{ erg s}^{-1}$ for haloes with $T_{\text{vir}} = 0.3 \text{ keV}$, assuming a preheated entropy similar to that which we adopt here. Thus, preheating can help to alleviate the X-ray halo problem for late-type galaxies.

2.4 Accretion of cooled clouds

Given the density and temperature profiles, we can estimate the cooling time scale once the metallicity of the gas is known. Figure 4 shows the ratio between the cooling time t_{cool} and the Hubble time t_H assuming that the gas has a metallicity $Z = 0.1Z_\odot$ (the cooling time is reduced by a factor of about 2 if we assume $Z = 0.3Z_\odot$). We used the cooling function given in Sutherland & Dopita (1993). Notice that the smaller the ratio t_{cool}/t_H , the more effective the cooling is. Effective cooling is expected when $t_{\text{cool}}/t_H \sim 1$. As one can see from the figure, cooling is more effective at low redshift. The main reason for this is that the gas density around dark haloes does not change very rapidly with redshift (and so the cooling time does not change rapidly) while the Hubble time increases with decreasing redshift. The situation is quite different in the absence of preheating, where the characteristic gas density changes with redshift as $(1+z)^3$ and cooling is always more effective at higher redshift. Note that once cooling becomes important, the gas can no longer be considered adiabatic. Thus, the adiabatic assumption may break down at low redshift. The ratio t_{cool}/t_H does not change significantly with radius at a given redshift, implying that the cooling efficiency is quite independent of radius. This is very different from what one obtains based on the assumption that gaseous haloes are (approximately) isothermal spheres, where gas cooling is always inside-out.

Because the cooling time is quite long for the preheated medium, most of the gas can remain in the hot phase. But some gas can cool due to radiative cooling. Since the preheated gas is expected to be clumpy, cooling is expected to start from regions where the gas density is enhanced, and a two-phase medium may develop due to thermal instabil-

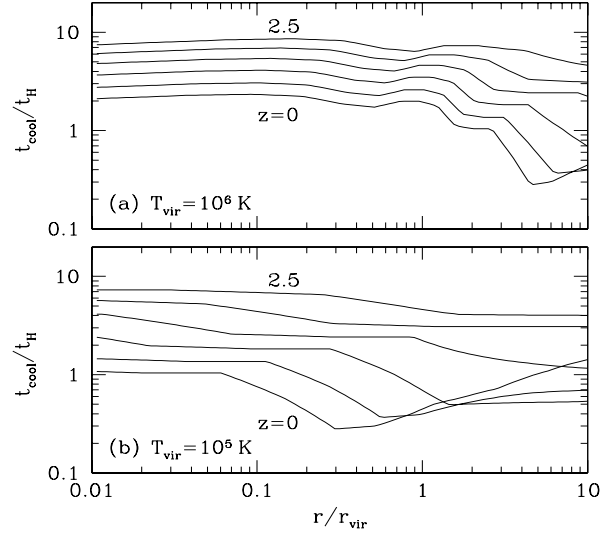


Figure 4. The ratio between cooling time and Hubble time of preheated gas around dark haloes. Results are shown for (a) a normal galaxy halo with $T_{\text{vir}} = 10^6$ K and (b) a dwarf galaxy halo with $T_{\text{vir}} = 10^5$ K.

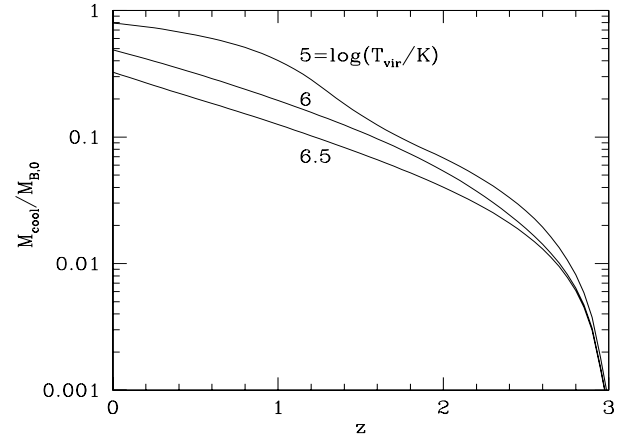


Figure 5. The mass fraction in cooled gas (defined as the ratio between the mass of cooled gas M_{cool} and $M_{B,0}$, with $M_{B,0}$ equal to f_B times the total halo mass at the present time) as a function of redshift in protogalaxy regions which were preheated at $z = 3$. The specific entropy is assumed to be $S_{100} = 1.0$ and the gas metallicity is assumed to be $0.1Z_\odot$. Results are shown for haloes with $T_{\text{vir}} = 10^5, 10^6$ and $10^{6.5}$ K.

ity, with the hot phase at the temperature set by preheating and a cold phase at $\sim 10^4$ K (below which radiative cooling may be inefficient, particularly in the presence of photoionization heating). The cold clouds produced in this way may be gravitationally accreted into dark haloes.

Since both the density and temperature of the gas may change with time as the dark halo grows, and since the medium is likely inhomogeneous and multi-phase, an accurate estimate of the amount of cold gas that can be accreted in a protogalaxy can be obtained only with the use of numerical simulations. Here we give an approximate estimate

based on simple assumptions. We assume that as a dark halo grows with time, its circular velocity V_c remains constant. For simplicity, we assume the dark halo mass profile is described by a singular isothermal sphere, and so its radius increases with time as $r_{\text{vir}} \propto 1/H(z)$ (see eq. 8). At any given time, most of the gas is assumed to be hot, with the gas density profile given by equations (12) and (13), while part of the gas in high-density regions cools. Assuming further that the total gas mass within a spherical mass shell does not change with time, we can estimate (at any given redshift) the cooling time using the equilibrium density and temperature of the mass shell in consideration. From the definition of the cooling time, the fraction of the gas that has cooled by redshift z can be estimated from

$$f_{\text{cool}}(z) \equiv \int \frac{dt}{t_{\text{cool}}} \\ \approx 1.5 \times 10^{-3} h^{-1} \left(\frac{\Omega_{\text{B},0} h^2}{0.02} \right) \\ \times \int_{z_{\text{ph}}}^z \frac{H_0 dt}{dz'} \frac{\Lambda_{-23}}{T_6} (1 + \delta) [1 - f_{\text{cool}}(z')] (1 + z')^3 dz', \quad (16)$$

where z_{ph} is the redshift at which the gas is preheated, and the factor $[1 - f_{\text{cool}}(z')]$ in the integrand takes into account the depletion of the hot gas due to cooling. Since the density of a fixed mass shell is known as a function of z in our model, we can obtain $f_{\text{cool}}(z)$ for each mass shell. We can then integrate over all the mass shells to obtain the total amount of gas that has cooled in the protogalaxy region by some redshift z . Figure 5 shows the ratio, $M_{\text{cool}}/M_{\text{B},0}$ (where $M_{\text{B},0}$ is equal to f_{B} times the total halo mass at the present time) as a function of z . Several important conclusions can be drawn from the figure. (i) In all cases, significant cooling occurs at low redshift, for the reasons discussed earlier in this subsection. (ii) For small haloes, rapid gas cooling occurs at $z \sim 1$ when the temperature of the preheated gas reaches the level $T \lesssim 2 \times 10^5$ K where the cooling rate peaks. In this case, the large amount of cooled gas may trigger episodes of star formation, which may in turn drive outflows and prevent further accretion of cooled gas. (iii) For large haloes, the fraction $M_{\text{cool}}/M_{\text{B},0}$ [which is roughly proportional to $(1 + z)^{-3/2}$ at low z] is significantly smaller than 1, and so only a fraction of the gas in the protogalaxy region can cool and be accreted.

3 GALAXY FORMATION IN A PREHEATED INTERGALACTIC MEDIUM

In the last section we have shown that gas accretion by galaxy haloes in a preheated medium has several distinct properties. In this section, we discuss the implications of such gas accretion for the formation of galaxies.

Based on the discussion in the last section, we may roughly divide stars in a galaxy into two populations: one formed in starbursts before preheating and the other formed due to the accretion of gas in the preheated medium. The relative importance of these two populations may determine the morphological type of the galaxy, because the early starbursts were likely to form a bulge component, while an extended disk can only form through gas accretion.

3.1 The formation of disk galaxies

As we have seen in Section 2, the gas accretion in a preheated medium by dark haloes occurs at rather low redshifts (more than half of the gas is accreted at $z \lesssim 1$). Thus, galaxy disks are expected to form late in this model. In fact, late formation of present-day galaxy disks is required in the standard model of disk formation (where disk size is determined by the specific angular momentum of dark haloes), because the formation at high redshifts (> 1) predicts disks that are too compact to match the observed sizes (e.g. MMW). The late formation of galaxy disks (relative to the bulges) may also be required in order to solve the G-dwarf problem (Ostriker & Thuan 1975).

Another important property of the disk formation in a preheated medium is that only part of the gas in a protogalaxy region can settle into a disk in the galaxy halo. Based on the discussion in Section 2, this fraction is about $f = 0.3 - 0.5$ for galaxy haloes, and so the ratio between disk mass and halo mass is $m_d \sim f \Omega_{\text{B},0} / \Omega_0 \sim 0.04 - 0.06$ (where we have assumed $\Omega_{\text{B},0} = 0.02 h^{-2}$, $\Omega_0 = 0.3$ and $h = 0.7$). This fraction is in fact required in the standard model of disk formation. Indeed, if all of the gas in a protogalaxy region can settle in the disk, then $m_d \sim 0.13$ in the standard Λ CDM model. Such a high value of m_d leads to too massive disks which have too peaked rotation curves and may be unstable (MMW). The model present here naturally leads to the required reduction.

In the standard model of disk formation, the specific angular momentum of disk material is assumed to be comparable to that of dark matter. Since disk material and dark matter is well mixed in a protogalaxy, this assumption may be valid before the collapse of the dark halo. However, in order for the assumption to hold for the formed disk, one has to make the assumption that there is no significant angular-momentum transfer from the disk material to dark matter during the formation of disks. As shown by the simulations of Weil et al. (1998), this requires the gas to remain in a diffuse form before it collapses into the final halo. This is exactly the case in the present model, where most of the gas remains in a hot, diffuse form until late time ($z \lesssim 1$) when the final halo collapses. Since this gas does not suffer the same dynamical friction as dark matter clumps, the final distribution of specific angular momentum of the gas may be different from that of the dark matter.

To see this point more clearly, we consider a simple case where a smaller halo, M_{vir} , merges into a larger halo, M'_{vir} . For simplicity, we assume the total mass profiles in both haloes are described by that of a singular isothermal sphere, while the gas distribution in the small halo is given by eq. (13). The smaller halo is taken to be always on a circular orbit as it sinks towards the center of the larger one due to dynamic friction. Because of tidal stripping, the outer part of the smaller halo will be truncated, and we estimate the truncating radius r_t on a orbit of radius r' by $\rho(< r_t) = \rho'(< r')$. For the assumed density profile, we have $r_t = (r_{\text{vir}}/r'_{\text{vir}})r'$, and the remaining mass of the smaller halo within r_t is $M(< r_t) = V_c^2 r_t / G$. For material on circular orbits in the bigger halo, the specific angular momentum is $j(r') = V'_c r'$. It is then easy to show that after merger the mass of dark matter that originated in M_{vir} with specific angular momentum smaller than j is

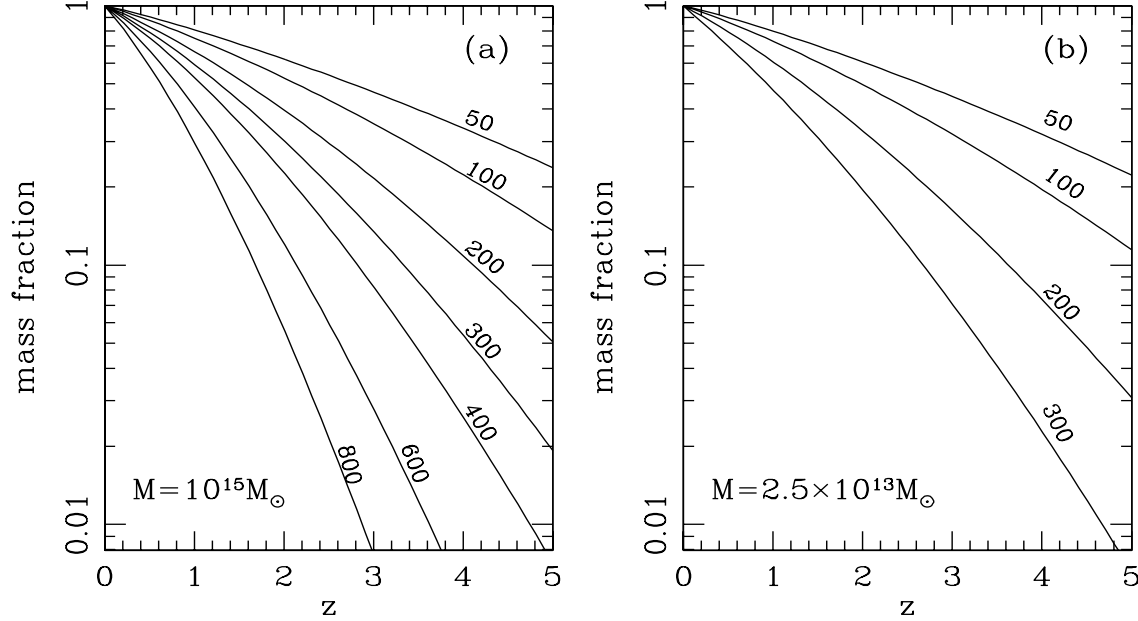


Figure 6. The fraction of the total halo mass M in progenitors with circular velocities exceeding V_c as a function of redshift. Panel (a) shows the results for a present-day rich cluster with mass $M = 10^{15} M_\odot$, while panel (b) shows the results for a present-day group with mass $M = 2.5 \times 10^{13} M_\odot$. The circular velocities of progenitors are labeled on the curves in units of km s^{-1} . The calculations are for the standard Λ CDM model based on the extended Press-Schechter formalism (e.g. Bond et al. 1991).

$$M(< j) = M_{\text{vir}} \frac{j}{j_{\text{vir}}}, \quad (17)$$

where $j_{\text{vir}} = V_c' r_{\text{vir}}'$. For the gas, the corresponding mass is given by

$$M_{\text{gas}}(< j) = \int_0^{r_j} 4\pi \rho_{\text{gas}}(r) r^2 dr, \quad (18)$$

where $\rho_{\text{gas}}(r)$ is the gas mass density around the smaller halo, and $r_j = r_{\text{vir}} j / j_{\text{vir}}$. For the gas density profile given by equation (13),

$$M_{\text{gas}}(< j) = 4\pi \bar{\rho}_{\text{gas}} r_{\text{vir}}^3 (1 + \alpha) \times \int_0^{j/j_{\text{vir}}} x^2 \left[1 - \frac{\alpha}{1 + \alpha} \ln x \right]^{3/2} dx, \quad (19)$$

where $\alpha \equiv (4/5) T_{\text{vir}} / (\mathcal{S} \bar{n}^{2/3})$. Since the logarithmic term changes only slowly with x , we have, to a good approximation,

$$M_{\text{gas}}(< j) \propto \left(\frac{j}{j_{\text{vir}}} \right)^3. \quad (20)$$

Numerically, we found that for $\alpha = 0.1$, $M_{\text{gas}}(< j) \propto j^{2.9}$ and for $\alpha = 10$, $M_{\text{gas}}(< j) \propto j^{2.6}$. Clearly this distribution is much steeper than that given by equation (17) for the dark matter. In fact, the shallower the gas density profile is, the steeper the dependence of $M_{\text{gas}}(< j)$ on j . Physically, because of the shallow density profile, most of the gas is stripped in the outer part of the bigger halo and so retains higher specific angular momentum; only a small fraction of the gas can sink to the inner part and lose a large amount of angular momentum. This effect exists wherever the gas distribution is more extended than the dark matter.

We emphasize that this effect remains even if we have multiple accretion events that occur with different angles and this will lead to a reduction in the net specific angular momentum of the accreted gas. However, the specific angular momentum of the gas will still be higher than that of the dark matter, if both are reduced by the same factor. This may help to solve the problem pointed out by Bullock et al. (2001) and van den Bosch et al. (2001) that the assumption that the gas and dark matter in dark haloes have the same angular-momentum distribution leads to too concentrated disks.

3.2 Formation of cluster galaxies and morphological segregations

As one can see from Figure 6, significant fraction of the total mass of a present-day rich cluster is already in group-sized systems with circular velocity $V_c \gtrsim 400 \text{ km s}^{-1}$ at $z \gtrsim 2$. These groups are expected to be associated with high-density peaks in a protocluster region, and so are likely to end up in the central part of a cluster. Since galaxy haloes cannot have accreted significant amount of gas from the preheated gas at $z > 1$ and since cooling of gas is already inefficient in such group haloes, we expect that galaxies which end up in the central part of clusters contain mainly old stars that have formed through starbursts before preheating. As the haloes of these galaxies merge, the stellar components also merge due to dynamical friction to form bigger galaxies. Such mergers of galaxies continue until the galaxies are incorporated into clusters in which dynamical friction is no longer effective. We identify this to be the formation path for giant ellipticals in clusters. This formation is in fact sim-

ilar to that in the standard model where cluster ellipticals are formed by mergers of galaxies (e.g. Kauffmann 1996). The effect of preheating is to suppress the formation of new stars, because gas accretion was prohibited after preheating. Since a group halo at $z \sim 1$ contains many smaller haloes at the time of preheating, the formation of a giant elliptical is expected to be a result of multiple mergers of stellar systems formed through early starbursts, and clusters ellipticals are therefore expected to contain mainly old stars. This early formation of elliptical galaxies (at least their stars) in gas-rich systems may be responsible for their tight colour-magnitude relation (e.g. Bower et al. 1992) and other properties which are distinct from present-day spiral galaxies (e.g. Ostriker 1980).

As one can also see from Figure 6, about 30% of the total mass of a present-day rich cluster remains in small haloes ($V_c \lesssim 200 \text{ km s}^{-1}$) at $z \lesssim 1$. This fraction is expected to end up in the outer part of the cluster. These haloes can accrete significant amount of gas before they are incorporated into larger systems. The accreted gas may form new stars on a disk around an old bulge, although young stars may also be added to the bulge either due to disk instability or due to the accretion of satellites containing young stellar component. If such systems merge into groups before being incorporated into the final cluster, the galaxies they contain may also merge, producing ellipticals with young stellar populations; otherwise they remain as spiral or S0 galaxies if their disks are not destroyed later in the cluster environment.

Similar discussion can be made for galaxy formation in smaller systems, such as present-day groups of galaxies. The only difference here is that, by definition, galaxy haloes can survive to later times before being incorporated into group haloes with $V_c \gtrsim 300 \text{ km s}^{-1}$ (see Fig. 6b) and so can accrete more gas to form disks. The mergers of such disks may also form elliptical galaxies, but unlike giant ellipticals in clusters, these ellipticals should contain a lot of younger stars. Since the merger progenitors here contain gaseous disks, such mergers can produce the tidal tails and starbursts observed at low redshifts.

If we use the disk-to-bulge ratio to represent the morphological type of a galaxy, the above discussion suggests that the gas content, stellar age and local environment of galaxies should change systematically along the morphology sequence. Late-type galaxies are formed in low-density regions where gas accretion lasts for a longer period, so they are gas richer, bluer and residing in lower density than early-type galaxies. This trend is qualitatively consistent with observations (e.g. Roberts & Haynes 1994; Dressler 1980; Postman & Geller 1984). However, quantitatively this prediction has to be studied taking into account of dynamical evolution and merging between galaxies. Such a detailed calculation in a cosmological context is clearly needed but is beyond the scope of this paper.

4 PREHEATING THE INTERGALACTIC MEDIUM

The preheating of the IGM has been discussed quite extensively in connection to the observed entropy excess in clusters and groups (Kaiser 1991; Evrard & Henry 1991; Ponman et al. 1999; Tozzi & Norman 2001 and references

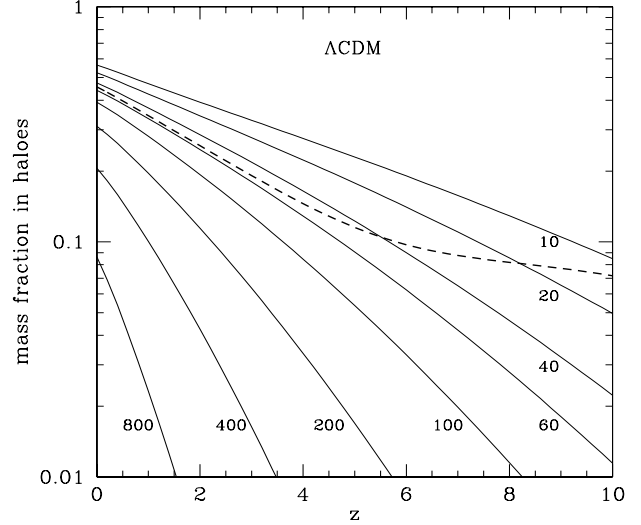


Figure 7. The mass fraction of the universe in haloes with circular velocities exceeding V_c (labeled on curves in units of km s^{-1}) as a function of redshift. The calculations use the halo mass function given in Sheth, Mo & Tormen (2001), and are for the standard ΛCDM cosmogony with $\Omega_0 = 0.3$, $\Omega_\Lambda = 0.7$, $h = 0.7$ and $\sigma_8 = 0.9$. The thick dashed curve shows the mass fraction in haloes which can trap photoionized gas [adopted from Gnedin (2000)].

therein). In this section we discuss further some points which are closely related to our discussion of galaxy formation.

4.1 Preheating by starbursts and AGNs

If we assume a stellar mass function (IMF) of the standard Salpeter form [$n(M)dM \propto M^{-2.35}dM$, for $0.1M_\odot < M < 50M_\odot$] and that each star of mass greater than $8M_\odot$ releases $10^{51} E_{51}$ erg in kinetic energy in a supernova explosion, the total energy output (E_{sn}) is related to the total amount of stars formed (M_\star) by

$$E_{\text{sn}} \approx 7.5 \times 10^{48} E_{51} (M_\star / M_\odot) \text{ erg}. \quad (21)$$

If a fraction ϵ of this energy is to heat gas with total mass M , each gas particle will gain an energy (in terms of temperature):

$$T_{\text{sn}} \sim 1.8 \times 10^7 \epsilon E_{51} \left(\frac{M_\star}{M} \right) \text{ K}. \quad (22)$$

The ratio between this temperature and that given by equation (3) is

$$\frac{T_{\text{sn}}}{T} \sim 410 \epsilon E_{51} \left(\frac{M_\star}{M} \right) S_{100}^{-1} (1 + \delta)^{-2/3} (1 + z)^{-2}. \quad (23)$$

If we take $\delta = 0$, $z = 3$ and $S_{100} = 1$, then $\epsilon M_\star / M \sim 0.04$.

X-ray observations of galaxy clusters show that the mass in stars is about 10% of the total mass in the X-ray gas (e.g. Böhringer 1995; Balogh et al. 2001). In this case $M_\star / M \sim 0.1$. A similar number can be obtained as follows. The observed mass density in stars is $\Omega_\star \sim 2 \times 10^{-3} h^{-1}$ and one-third to a half of this may be in old stellar systems, such as ellipticals and bulges (e.g. Fukugita, Hogan & Peebles 1998). If we take the standard ΛCDM model,

the fraction of cosmic mass in protogalaxy regions (i.e. regions which form haloes with circular speeds $\sim 200 \text{ km s}^{-1}$ at the present time) is about 0.3 (see Figure 7). Thus $M_{\star, \text{old}}/M \sim \Omega_{\star, \text{old}}/(0.3\Omega_{\text{B},0}) \sim 0.1$. If the heating of the IGM were all due to star formation, an efficiency $\epsilon \sim 0.4$ would be required. This efficiency is higher than usually assumed (e.g. Valageas & Silk 1999; Wu, Fabian & Nulsen 2000; Kravtsov & Yepes 2000). However, an efficiency as high as this is in fact indicated by observations of supernova-driven winds in local starburst galaxies (Heckman et al. 2000). Thus, if most stars at high redshifts were formed in systems reminiscent of local starbursts, as suggested by the observed properties (high star-formation rate, compact size) of high-redshift galaxies (see Heckman 2001 and references therein), the stellar energy sources may be sufficient to preheat the IGM to the required level. More quantitatively, the observed mass-outflow rate in a local starburst is usually comparable to the star-formation rate, and the wind velocity is typically $500 - 600 \text{ km s}^{-1}$. If the kinetic energy of the wind is to be thermalized in the IGM, it can heat as much as ten times M_{wind} (the mass of the wind) of the IGM to the required temperature at $z \sim 3$ [see equation (3)]. Since $M_{\text{wind}} \sim M_{\star}$, the total preheated mass is $M \sim 10M_{\star}$, consistent with the star/gas mass ratio estimated above.

An alternative energy source for the preheating may be AGNs. For example, radio galaxies can provide a total energy output about two orders of magnitude larger than stellar sources, and so have the potential to heat the IGM to the required level (e.g. Inoue & Sasaki 2001). Since the mass of central black hole (which powers the AGN) is found to be proportional to the bulge mass in a galaxy (e.g. Magorrian et al. 1998; Gebhardt et al. 2000), the energy output from AGNs in a region large enough to contain many AGNs should be roughly proportional to the energy output from stellar sources. Thus, the inclusion of additional energy output from AGNs is equivalent to increasing the value of ϵ . The uncertainty here is again how large a fraction of the total energy released by AGNs can be thermalized in the IGM.

4.2 The epoch of preheating

If the preheating was indeed done by activity associated with star formation and AGNs, the likely epoch for preheating is when the star-formation and AGN activity peaks. The observed comoving number density of AGNs peaks around $z = 2$ to 3 (Shaver et al. 1996). The star formation history in the universe can be inferred from the observed $\dot{\Omega}_{\star}(z)$ which is the change rate of the density parameter of stars. Observations showed that $\dot{\Omega}_{\star}$ remains approximately constant ($\sim 10^{-3} \text{ Gyr}^{-1}$) in the redshift range $z = 2 - 4$, and decreases rapidly with decreasing z at $z < 1$ (e.g. Blain et al. 1999). For the Λ CDM model, the age of the universe at $z \sim 3$ is about 1.5 Gyr, and so the mass density parameter of all stars formed before $z = 3$ is $\Omega_{\star} \sim 10^{-3}$, consistent with the total amount of stars observed in old stellar systems. Thus, if the mass of gas that can be heated up to the required entropy is about ten times that of the old stars, the density parameter of the heated gas is $\Omega_{\text{gas}} \sim 0.01 \sim 0.2\Omega_{\text{B},0}$, which is similar to the gas mass in proto-group regions (see Fig. 7). From these considerations, we see that the epoch of preheating is likely to be around $z = 2$ to 3 .

Similar conclusion can be drawn from theoretical considerations. As shown in Figure 6a, about 20% of the total mass of a present-day cluster is already in progenitors with circular velocities $V_c \gtrsim 200 \text{ km s}^{-1}$ at $z \sim 3$. This fraction is only slightly smaller for a present-day group (see Fig. 6b). Most systems that have formed by redshift 3 will suffer a major merger in a Hubble time (see Fig. 14 in Shu, Mao & Mo 2001), and so most of them may form stars in starbursts. If half of the gas in these systems forms stars, and the other half escapes as outflows with the escaping velocity, $v_{\text{esc}} \sim 3V_c$ [where we assumed a singular isothermal sphere and the gas escapes at roughly one disk scale length, cf. equation (12) in MMW and equation (2-192) in Binney & Tremaine (1987)], then the IGM in the protogroup (or protocluster) regions can be preheated to the required level at $z \sim 3$. As one can see from Fig 6, about half of the total mass of a present-day cluster is in progenitors with circular velocities $V_c \lesssim 50 \text{ km s}^{-1}$ at $z \sim 3$. Since such haloes cannot trap much gas in the presence of the general UV background (e.g. Efstathiou 1992; Gnedin 2000), more than half of the protocluster (protogroup) gas must be in diffuse form. Thus, most of the gas to be heated is in a diffuse medium outside collapsed haloes. The situation here is different from that in previous feedback schemes without preheating, where the goal is to heat up and get rid of the gas that has already been assembled into galaxies or galactic haloes.

In reality, the time of preheating must be different in different regions. In high-density regions where a significant fraction of the mass was already in galactic haloes at high redshifts, the time of preheating is expected to be early, while in low-density regions where galaxy haloes form at low redshifts, the time of preheating is expected to be late. In regions where starbursts never occur, the IGM is not preheated. A detailed modelling of how and when different regions in the universe were heated up depends on how the heating sources form in the cosmic density field and how their energy is thermalized in the IGM. This is a complicated problem and will not be considered in this paper.

4.3 Preserving the Ly α forest

If all of the IGM were heated to the temperature implied above, then there would be no photoionized gas to produce the observed Ly α forest. This is not allowed, because the Ly α forest is observed. However, the above discussion does not require the preheating to be everywhere in the IGM. In fact, in order to explain the observed entropy excess, it is only necessary to preheat the gas which ends up in present-day groups and clusters. Since groups and clusters are places where vigorous star-formation and AGN activities are expected in the early time, it is also *likely* that preheating occurred mainly in protocluster (protogroup) regions. In fact, star-forming galaxies at high redshifts, such as Lyman-break galaxies and sub-mm sources observed at $z \sim 3$, are expected to be located in high density regions which will eventually be in present-day groups and clusters (e.g. Mo, Mao & White 1999, and references therein). It is therefore possible that the IGM in the low density regions, which may be responsible for the observed Ly α forest, is not affected significantly, while the high density regions are heated. To demonstrate that this is likely the case, we can estimate the fraction of the total mass which is in systems more massive than present-day

groups (i.e. with circular speeds $\gtrsim 400 \text{ km s}^{-1}$). As shown in Figure 7, this fraction is about 20% in standard Λ CDM. In fact more than half of the total mass is in systems which are too small to trap photoionized gas. These systems are outside protogalaxy regions, and so may not be influenced significantly if preheating is confined to proto-group regions by the associated gravitational potentials.

Of course, preheating may produce some effects that can be observed in the Ly α forest (Theuns, Mo & Shaye 2001). If the preheating is due to supernova-driven winds from starbursts, some of the metals ejected by the heating sources may leak to the Lyman forest and contaminate it, although most of the metals may be hidden in the hot phase. This may in fact be the origin of the ‘missing metal’ problem that the total amount of metals observed at $z \sim 3$ seems smaller than that expected from the observed star formation history (e.g. Pettini 1999).

5 DISCUSSION AND SUMMARY

In this paper, we have outlined a scenario of star-formation feedback in which the IGM in galaxy-forming regions was preheated. The preheating of the intergalactic medium in high-density regions of the cosmic density field may be responsible for the entropy excess observed in low-mass clusters of galaxies and yet may not destroy the bulk of the Ly α forest. The subsequent galaxy formation in preheated media is different from that in models without preheating, because the gas component no longer follows the bottom-up clustering hierarchy of the dark matter component on galaxy scales. Because of the initial entropy, the hot gas around a galaxy halo has a very shallow profile, and so emits only weakly in X-ray. This may be the reason why extended X-ray haloes are not yet detected around spiral galaxies. Radiative cooling of the preheated gas around galaxies may become more significant at lower redshift when the cosmic time becomes longer. Unlike in the absence of preheating, where cooling is always inside-out in a halo, the cooling efficiency in a preheated halo does not change rapidly with radius. Because of thermal instability, the cooled gas may form cold clouds which can then sink toward the centre in the potential wells of galaxy haloes to form galaxy disks. The total amount of the gas that a galaxy halo can accrete by the present time is significantly smaller than the total gas in the protogalaxy region. Since most gas is accreted in diffuse clouds, the gas may not lose angular momentum to dark matter due to dynamical friction. Cluster ellipticals are produced by the mergers of stellar systems formed prior to the preheating, because these systems cannot accrete much gas from the preheated medium to form new stars before they are incorporated into large haloes where gas cooling is inefficient. Large galaxy disks form in low-density environments where accretion of gas can continue to the present time. Mergers of such disks may trigger new starbursts and form field ellipticals. Thus, the stellar age, gas content, and local environment of galaxies are expected to change systematically along the morphology sequence.

The scenario proposed here can be tested by observations of its assumptions and predictions. If part of the IGM was indeed heated up to a high temperature, we may hope to find some signatures of such heating in the Ly α forest (The-

uns, Mo & Schaye 2001). Since the preheating is most likely in regions of vigorous star formation, observations of the Ly α forest near star-forming galaxies, such as the Lyman-break population (e.g. Steidel et al. 1999), are important for probing the properties of the preheating. Because the preheated gas contains metals and is at a temperature much higher than 10^4 K , observations of absorption lines of collisionally ionized metal species (e.g. O VI) are also important. Another test may come from observations of the diffuse X-ray emission from spiral-galaxy haloes. As discussed in Section 2, current observational results are still too uncertain to provide stringent constraints. Future observations from the more sensitive detectors, such as XMM and Chandra may be used to probe the gaseous haloes predicted here.

Yet another test of the model may come from observations of the cold gas around galaxy haloes. An important probe here is provided by QSO absorption line systems associated with low-redshift galaxies. Such systems have been observed. For example, normal galaxies at moderate redshifts ($z \lesssim 1$) are observed to produce strong MgII systems whenever the impact parameter to a QSO sightline is smaller than $\sim 40 h^{-1} \text{ kpc}$ (Steidel 1995 and references therein), suggesting that each galaxy may possess a halo of cold clouds. Weaker MgII systems are also observed to be associated with galaxies at larger impact parameters (e.g. Rigby, Charlton & Churchill 2002). These absorption systems may be produced by the cooling clouds predicted in the present model. Indeed, there are theoretical investigations along this line (e.g. Mo 1994; Mo & Miralda-Escude 1996; Lin et al. 2000). Assuming that strong MgII systems are produced by gas clouds cooling from and pressure-confined by hot haloes similar to those considered here, Mo & Miralda-Escude found that many of the observed properties of the absorber/galaxy systems can be reproduced. Clearly, more observations of this kind can give stringent constraints on the gaseous galaxy haloes we are proposing here.

On the theoretical side, there are several important issues for which further investigations are required. For the preheating, we need a physical model to predict how the IGM was heated. For simplicity, we have modelled the preheated IGM as a uniform medium. This is clearly a simplification, as the density contrast is likely a smooth function of radius, decreasing from the center of the preheating energy sources (bulges or AGNs) to the preheated IGM. Also if the preheating is accompanied by outflows, the interplay between outflows and gas accretion needs to be modelled in detail. Some of these issues are best addressed using numerical simulations. Finally, we also need to incorporate the present scenario of galaxy formation into realistic cosmological models to make detailed predictions for the properties of the galaxy population. We intend to return to some of these issues in future papers.

ACKNOWLEDGEMENT

We thank James Bullock, Jerry Ostriker, Frank van den Bosch, Simon White and the referee, Peter Thomas, for helpful comments and suggestions.

REFERENCES

- Avila-Reese V., Firmani C., Hernandez X., 1998, *ApJ*, 505, 37
- Balogh M. L., Pearce F. R., Bower R. G., Kay S. T., 2001, *MNRAS*, 236, 1288
- Benson A.J., Bower R.G., Frenk C.S., White S.D.M., 2000, *MNRAS*, 314, 557
- Binney J., Tremaine S., 1987, *Galactic Dynamics*. Princeton Univ. Press, Princeton, NJ
- Blain A.W., Small I., Ivison R.J., Kneib J.P., 1999, *MNRAS*, 302, 632
- Blumenthal G.R., Faber S.M., Primack J.R., Rees M.J., 1984, *Nat*, 311, 517
- Böhringer H., 1995, *Ann. N. Y. Acad. Sci.*, 759, 67
- Bond J.R., Cole S., Efstathiou G., Kaiser N., 1991, *ApJ*, 379, 440
- Bower R.G., Lucey J.R., Ellis R.S., 1992, *MNRAS*, 254, 601
- Brighenti F., Mathews W.G., 1999, *ApJ*, 512, 65
- Bullock J.S., Dekel A., Kolatt T.S., Kravtsov A.V., Klypin A.A., Porciani C., Primack J.R., 2001, *ApJ*, 555, 240
- Cole S., Aragon-Salamanca A., Frenk C.S., Navarro J.F., Zepf S.E., 1994, *MNRAS*, 271, 781
- Dalcanton J.J., Spergel D.N., Summers, F.J., 1997, *ApJ*, 482, 659
- de Bernardis P., et al., 2002, *ApJ*, 564, 559
- Dekel A., Silk J., 1986, *ApJ*, 303, 39
- Dressler A., 1980, *ApJ*, 236, 35
- Efstathiou G., 1992, *MNRAS*, 256, P43
- Ettori S., Fabian A.C., 1999, *MNRAS*, 305, 834
- Evrard A.E., Henry J.P., 1991, *ApJ*, 383, 95
- Fall S.M., Efstathiou G., 1980, *MNRAS*, 193, 189
- Fukugita M., Hogan C. Peebles P.J.E., 1998, 503, 518
- Gebhardt K., et al. 2000, *ApJ*, 539, L13
- Gnedin N.Y., 2000, *ApJ*, 542, 535
- Heavens A.F., Jimenez R., 1999, *MNRAS*, 305, 770
- Heckman T.M., 2001, in Hibbard J.E., Rupen M., van Gorkom J.H., eds., *Gas and Galaxy Evolution*, ASP 240, p.345 0, *astro-ph/0009075*
- Heckman T.M., Lehnert M.D., Strickland D.K., Armus L., 2000, *ApJS*, 129, 493
- Inoue S., Sasaki S., 2001, *ApJ*, 562, 618
- Kaiser N., 1991, *ApJ*, 383, 104
- Kauffmann G., 1996, 281, 487
- Kauffmann G., White S.D.M., Guiderdoni B., 1993, *MNRAS*, 264, 201
- Kauffmann G., Colberg J.M., Diaferio A., White S.D.M., 1999, *MNRAS*, 303, 188
- Kravtsov A.V., Yepes G., 2000, *MNRAS*, 318, 227
- Larson R.B., 1974, *MNRAS*, 169, 229
- Lin W.P., Börner G., Mo H.J., 2000, *MNRAS*, 319, 517
- Lloyd-Davies E. J., Ponman T.J., Cannon, D. B., 2000, *MNRAS*, 315, 689
- Magorrian J., et al. 1998, *AJ*, 115, 2285
- Mo H.J., 1994, *MNRAS*, 269, L49
- Mo H.J., Mao S., 2000, *MNRAS*, 318, 163
- Mo H.J., Mao S., White S.D.M., 1998, *MNRAS*, 295, 319 (MMW)
- Mo H.J., Mao S., White S.D.M., 1999, *MNRAS*, 304, 175
- Mo H.J., Miralda-Escude J., 1996, *ApJ*, 469, 589
- Navarro J.F., Steinmetz M., 2000, *ApJ*, 538, 477
- Navarro J.F., White S.D.M., 1994, *MNRAS*, 267, 401
- Navarro J.F., Frenk C.S., White S.D.M., 1997, *ApJ*, 490, 493
- Nulsen P.E.J., Fabian A.C., 1995, 277, 561
- Nulsen P.E.J., Fabian A.C., 1997, 291, 425
- O'Meara J.M., Tytler D., Kirkman D., Suzuki N., Prochaska J. X., Lubin D., Wolfe A.M., 2001, *ApJ*, 552, 718
- Ostriker J.P., 1980, *Comments on Astrophys.*, 8, 177
- Ostriker J.P., Thuan T.X., 1975, *ApJ*, 202, 353
- Peebles P.J.E. 1982, *ApJ*, 263, L1
- Pettini M., 1999, in *Chemical Evolution from Zero to High Redshifts*, eds. J. Walsh & M. Rosa (Berlin: Springer), 233
- Ponman T.J., Cannon, D.B., Navarro J.F., 1999, *Nat.*, 397, 135
- Postman M., Geller M.J., 1984, *ApJ*, 281, 95
- Rigby J.R., Charlton J.C., Churchill C.W., 2002, *ApJ*, 565, 743
- Roberts M.S., Haynes M.P., 1994, *ARA&A*, 32, 115
- Shaver P.A., Wall J.V., Kellermann K.I., Jackson C.A., Hawkins M.R.S., 1996, *Nat.*, 384, 439
- Sheth R.K., Mo H.J., Tormen G., 2001, *MNRAS*, 323, 1
- Shu C., Mao S., Mo H.J., 2001, *MNRAS*, 327, 895
- Somerville R.S., Primack J.R., 1999, *MNRAS*, 310, 1087
- Sommer-Larsen J., Gelato S., Vedel H., 1999, *ApJ*, 519, 501
- Steidel C., Adelberger K.L., Dickinson M., Giavalisco M., Pettini M., 1999, *astro-ph/9812167*
- Steidel C.C., 1995, in *QSO Absorption Lines*, ed. G. Meylan (Berlin: Springer) 137
- Sutherland R.S., Dopita M.A., 1993, *ApJS*, 88, 253
- Theuns T., Mo H.J., Schaye J., 2001, *MNRAS*, 321, 450
- Tozzi P., Norman C., 2001, *ApJ*, 546, 63
- Tozzi P., Scharf, C., Norman C., 2000, *ApJ*, 542, 106
- Valageas P., Silk J., 1999, *A&A*, 350, 725
- van den Bosch F.C., 2000, *ApJ*, 530, 177
- van den Bosch F.C., Burkert A., Swaters R.A., 2001, *MNRAS*, 326, 1205
- Weil M.L., Eke V.R., Efstathiou G., 1998, *MNRAS*, 300, 773
- White S.D.M., Frenk C., 1991, *ApJ*, 379, 52
- White S.D.M., Rees M.J., 1978, *MNRAS*, 183, 341
- White S.D.M., Navarro, J.F., Evrard A.E., Frenk C., 1993, *Nat*, 366, 429
- Wu K.K.S., Fabian A.C., Nulsen P.E.J., 2000, *MNRAS*, 318, 889